RSC Publishing Faraday Discussions

Localization of transmembrane multiblock amphiphilic molecules in phase-separated vesicles

Journal:	*Faraday Discussions*
Manuscript ID	FD-ART-02-2018-000022.R1
Article Type:	Paper
Date Submitted by the Author:	20-Mar-2018

Complete List of Authors:	Kinbara, Kazushi; Tokyo Institute of Technology, School of Life Science and Technology Umetsu, Kaori; Tohoku University, Institute of Multidisciplinary Research for Advanced Materials Sonobe, Hiroki; Tokyo Institute of Technology, School of Life Science and Technology Muraoka, Takahiro; Tokyo University of Agriculture and Technology, Graduate School of Engineerin Shimokawa, Naofumi; Japan Advanced Institute of Science and Technology, School of Materials Science Takagi, Masahiro; Japan Advanced Institute of Science and Technology, School of Materials Science

Journal Name

ARTICLE

Localization of transmembrane multiblock amphiphilic molecules in phase-separated vesicles

Received 00th January 20xx,
Accepted 00th January 20xx

DOI: 10.1039/x0xx00000x

www.rsc.org/

Kazushi Kinbara,*[a] Kaori Umetsu,[b] Hiroki Sonobe,[a] Takahiro Muraoka,[a†] Naofumi Shimokawa,[c] and Masahiro Takagi[c]

A series of triblock amphiphilic molecules, bearing hydrophilic PEG chains at the both ends of the long aromatic hydrophobic moieties were obtained serendipitously. The molecules involve linearly connected diarylethyne and diarylbutadiyne units, which show charcteristic emissions upon excitation by UV lights. These emissions showed red-shifts upon increase in the solvent polarity, where the shifts are larger for the molecules with longer aromatic moieties. Distribution of these molecules in the phase-separated membranes cosisting of DOPC/DPPC/cholesterol were studied by fluorescence microscopy. It was found that most compounds, except for that having the longest hyrdophobic unit, were seletcively distributed in Ld phase consiting mainly of DOPC. Interestingly, some of them were suggested to encourage delocalization of cholesterol in both Lo and Ld phases.

Introduction

Membrane proteins have versatile functions, which play vital roles in the living systems.[1] One of the important functions of such membrane proteins is the control of permeability of substances, namely, formation of the channels or transporters.[2] Meanwhile, development of synthetic molecules, which have capability to pass the ions through the membranes like the membrane proteins, has been attracting long-term attention.[3–9] In association with this, we have been involved in the development of multiblock amphiphilic molecules as synthetic mimics of multipass transmembrane (MTM) proteins, which exhibit a characteristic structural motif advantageous for construction of stimuli-responsive systems.[10-14] Indeed, we have succeeded in construction of supramolecular ion channels by multiblock molecules with alternately aligned hydrophilic and planar aromatic hydrophobic units.[11] Thereafter, this molecular design concept could successfully be applied for construction of ligand-gated ion channels.[12] More recently, we found that the multiblock molecules **1mer-bpy** and **3mer-bpy** with non-planar aromatic units could form ion-channels sensitive to the osmotic pressure, namely membrane tension.[14] This is likely due to the rather weak stacking of aromatic units in the lipid bilayer, where the mode of stacking could alter according to the change in the membrane tension, and probably the dynamics of the lipid molecules in the membranes.

In relation to the dynamic feature of the membranes, domain formation in the membranes, as a result of lateral phase-separation, is a topic of increasing interest. In a typical example, a lipid bilayer consisting of unsaturated and saturated lipids, such as 1,2-Dioleoyl-sn-glycero-3-phosphocholine (DOPC) and 1,2-Dihexadecanoyl-sn-glycero-3-phosphocholine (DPPC) undergoes phase separation in the presence of cholesterol.[15-19] The domains are separated into

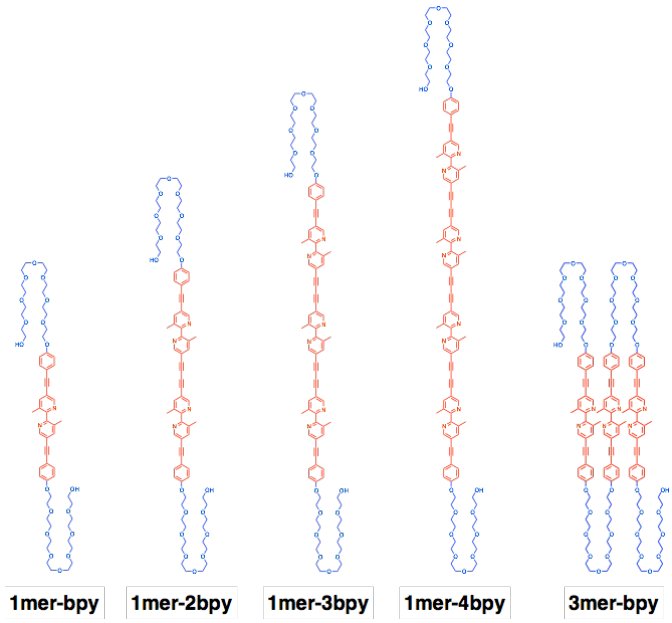

Figure 1. Structures of multiblock amphiphiles.

[a] School of Life Science and Technology, Tokyo Institute of Technology 4259 B58, Nagatsuta-cho, Midori-ku, Yokohama 226-8501, Japan.
[b] Institute of Multidisciplinary Research for Advanced Materials, Tohoku University, 2-1-1 Katahira, Aoba-ku, Sendai 980-8577, Japan.
[c] School of Materials Science, Japan Advanced Institute of Science and Technology, 1-1 Asahidai, Nomi, Ishikawa 923-1292, Japan.
† Present address: Institute of Global Innovation Research, Tokyo University of Agriculture and Technology, 2-24-16 Naka-cho, Koganei-shi, 228 Tokyo 184-8588, Japan.

DOPC-rich liquid crystalline domain (Ld phase) and DPPC/cholesterol-rich gel domain (Lo phase), where Ld phase is more fluid than Lo phase. This phase separation phenomena is regarded as a model of lipid-rafts formation in the cell membranes, which is now considered to play significant roles in regulation of the activity of the membrane proteins.[20-24] Thus, it is important to know the distribution of the synthetic molecules and their effect on the membrane property.

During the synthesis of **1mer-bpy**, we serendipitously obtained a series of multiblock compounds **1mer-2bpy**, **1mer-3bpy**, and **1mer-4bpy**, in addition to **1mer-bpy** (Figure 1). These compounds have different lengths of hydrophobic units with similar structures, while keeping the same hydrophilic units, and are suitable to see the effect of the length of the hydrophobic units on the behaviors in the lipid bilayers with different phases. Here we report distribution of these molecules in the phase-separated vesicles consisting of DOPC, DPPC, and cholesterol (Chol), and their influence on the membrane compositions.

Results and discussion

Synthesis of 1mer-2bpy, 1mer-3bpy, 1mer-4bpy.

As reported in our previous work, **1mer-bpy** was synthesized by Sonogashira-Hagihara cross coupling reaction between[25] bisethynyl-2,2'-bipyridine (**1**) and iodobenzene (**2**) bearing a hydrophilic tail at the *para*-position, using $Pd(PPh_3)_4$ and CuI (Figure 2). In this reaction, in addition to the target product **1mer-bpy**, **1mer-2bpy**, **1mer-3bpy**, and **1mer-4bpy** were also obtained as by-products, in 9%, 5% and 0.4%, yields respectively. It is likely that the oxidative coupling reaction between the alkynyl groups took place along with the cross coupling, which formed elongated aromatic moieties.

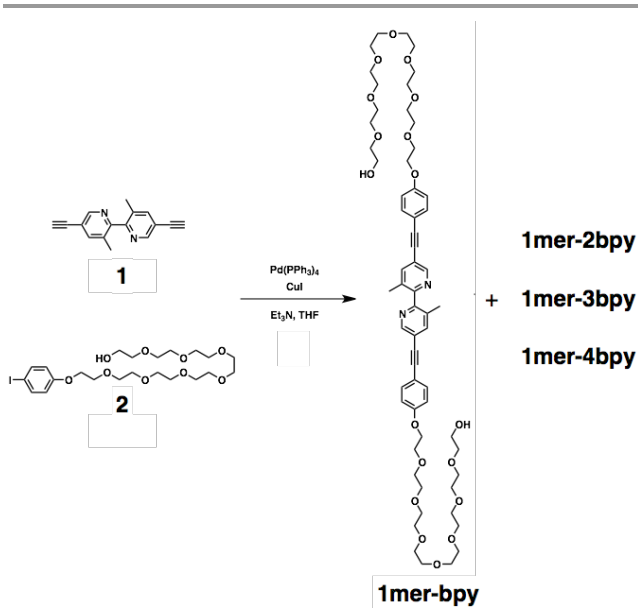

Figure 2. Synthesis of **1mer-bpy, 1mer-2bpy**, **1mer-3bpy**, and **1mer-4bpy** by Sonogashira-Hagihara cross coupling reaction between **1** and **2**.

Spectroscopic properties of 1mer-bpy, 1mer-2bpy, 1mer-3bpy, and 1mer-4bpy.

At first, we investigated the spectroscopic properties of **1mer-bpy**, **1mer-2bpy**, **1mer-3bpy**, and **1mer-4bpy** in solutions (Figures 3 and 4). In the UV-vis absorption spectrum, **1mer-bpy** showed absorption bands around 323 nm in CH_2Cl_2 (Figure 3a, red). Upon excitation at 323 nm, an emission band was observed at 410 nm (Figure 3e, red). In the case of **1mer-2bpy**, the absorption band slightly red-shifted to 328 nm with a shoulder around 340 nm (Figure 3b, red). The excitation at 328 nm resulted in the emission at 427 nm (Figure 3f, red). The excitation spectra corresponding to this emission band showed two bands at 331 and 342 nm (Figure 3j, red). These bands likely correspond to the excitation at the diarylethyne and diarylbutadiyne units, respectively. In the case of **1mer-3bpy**, two absorption bands were distinctively observed at 329

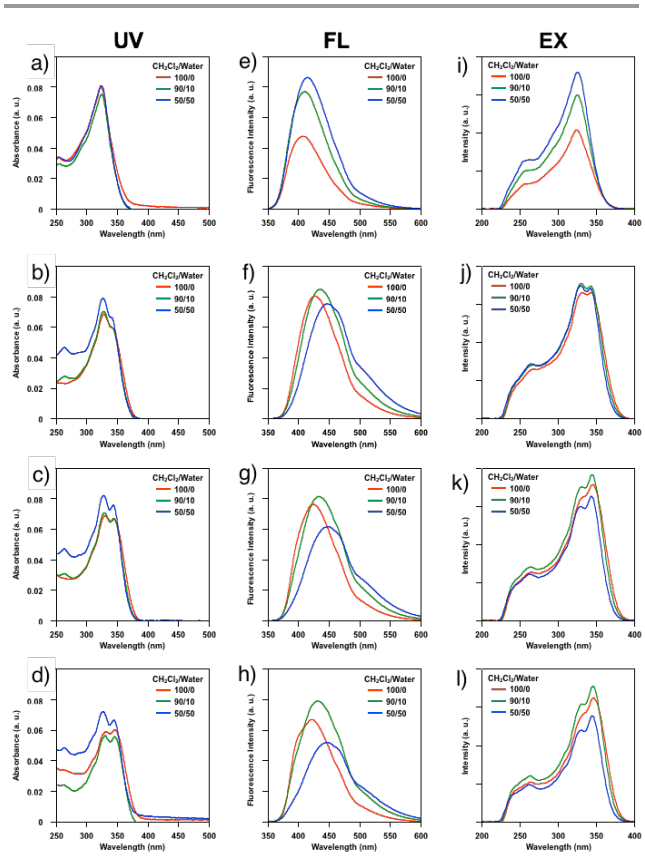

Figure 3. UV-vis, fluorescence, and excitation spectra of a), e), i) **1mer-bpy,** b), f), j) **1mer-2bpy**, c), g), k) **1mer-3bpy**, and d), h), l) **1mer-4bpy**. Solvents: red; CH_2Cl_2, green; CH_2Cl_2/water =9/1, blue; CH_2Cl_2/water =1/1. e)–h) Excitation wavelength λ_{ex} in CH_2Cl_2: 324, 328, 329, and 345 nm for **1mer-bpy, 1mer-2bpy**, **1mer-3bpy**, and **1mer-4bpy,** respectively; CH_2Cl_2/MeOH = 9/1; 325, 327, 329, and 346 nm for **1mer-bpy, 1mer-2bpy**, **1mer-3bpy**, and **1mer-4bpy,** respectively; CH_2Cl_2/MeOH = 1/1; 325, 326, 327, and 344 nm for **1mer-bpy, 1mer-2bpy**, **1mer-3bpy**, and **1mer-4bpy,** respectively. I)–l) Emission wavelength λ_{em} in CH_2Cl_2: 409, 427, 425, and 422 nm for **1mer-bpy, 1mer-2bpy**, **1mer-3bpy**, **1mer-4bpy,** respectively; CH_2Cl_2/MeOH = 9/1: 413, 434, 431, and 430 nm for **1mer-bpy, 1mer-2bpy**, **1mer-3bpy**, and **1mer-4bpy,** respectively; CH_2Cl_2/MeOH = 1/1: 417, 446, 449, and 444 nm for **1mer-bpy, 1mer-2bpy**, **1mer-3bpy**, and **1mer-4bpy,** respectively.

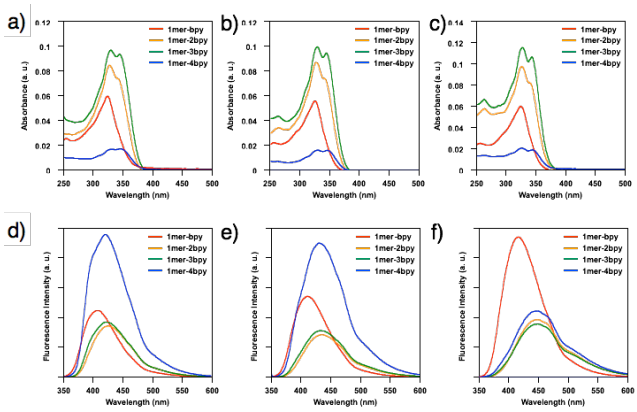

Figure 4. Overlapping a)-c) UV-vis absorption and d)-f) fluorescent spectra of **1mer-bpy, 1mer-2bpy**, **1mer-3bpy**, and **1mer-4bpy**, in a), d) CH_2Cl_2, b), e) CH_2Cl_2/MeOH = 9:1, and c), f) CH_2Cl_2/MeOH = 5/5. The conditions for the measurement are described in Figure 3.

and 344 nm (Figure 3c, red), and excitation at these bands resulted in the emission at 424 nm (Figure 3g, red). The excitation spectra for this emission band showed the highest peak at 346 nm (Figure 3k, red). Likewise, **1mer-4bpy** showed absorption bands at 334 and 345 nm (Figure 3d, red), where excitation at these absorption bands gave a 422 nm emission, (Figure 3h, red) respectively. These results suggest that the major chromophores of these molecules are diarylethyne and diarylbutadiyne units, which are likely to be excited separately to give the same excited state.

When the polarity of the solvent was increased by addition of MeOH, the absorption spectra showed slight red-shifts (Figure 4). Meanwhile, the emission spectra are more sensitive to the polarity. In the case of **1mer-2bpy**, the emission shifted from 407 to 415 nm. The emission of **1mer-4bpy** shifted from 422 to 445 nm. The conformation of the molecules at the excited state, including diarylbutadiyne units, is considered to be more sensitive to the polarity of the solvent.

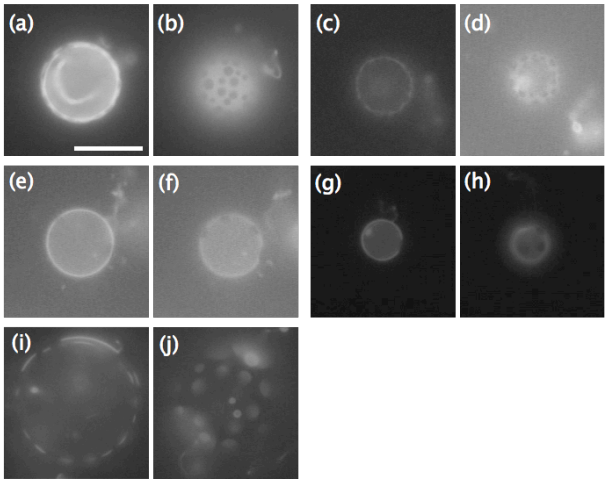

Figure 5. Fluorescence microscopic images of GUVs labelled by Rhodamine-DHPE in the presence of a), b) **1mer-bpy**, c), d) **1mer-2bpy**, e), f) **1mer-3bpy**, g), h) **1mer-4bpy**, and i), j) **3mer-bpy**. DOPC/DPPC/Chol/multiblolck amphiphile = 40/40/20/10. λ_{ex} = 530-550 nm. Scale bar: 10 µm.

Fluorescence microscopic observation of DOPC/DPPC/Chol/multiblock-amphiphile GUVs in the presence of rhodamine-DHPE.

The phase separation feature of the vesicles consisting of DOPC, DPPC and Chol is given by the ternary phase diagram. We decided to use the condition of DOPC/DPPC/cholesterol = 40/40/20, which is reported to form Lo/Ld type phase separation at an ambient temperature. It is known that Lo phase mainly consists of DPPC and cholesterol, while Ld phase mainly contains DOPC. We mixed **1mer-bpy, 1mer-2bpy**, **1mer-3bpy**, **1mer-4bpy**, and **3mer-bpy**, with the lipid mixtures in a ratio of DOPC/DPPC/cholesterol/multiblock-amphiphile = 40/40/20/10.

We added rhodamine B 1,2-dihexadecanoyl-sn-glycero-3-phosphoethanolamine (**rhodamine-DHPE**) in the giant unilamellar vesicles (GUVs), which is known to delocalize in the Ld phase of DOPC. Fluorescent microscopy of the vesicles observed at the emission corresponding to rhodamine clearly displayed the phase-separated vesicles in each case (Figure 5). This indicates that the phase separation occurs at this composition even in the presence of **1mer-bpy, 1mer-2bpy**, **1mer-3bpy**, **1mer-4bpy**, and **3mer-bpy**.

Fluorescence microscopic observation of DOPC/DPPC/cholesterol/multiblock-amphiphile GUVs without fluorescence-labelled lipids.

Next, we conducted the fluorescent microscopy in the absence of labelled lipids, to directly observe the distribution of **1mer-bpy, 1mer-2bpy**, **1mer-3bpy**, **1mer-4bpy**, and **3mer-bpy** in GUVs. After the existence of GUV was confirmed by phase contrast images, fluorescence images were observed at the excitation wavelength of 330–385 nm, corresponding to the absorption wavelength of these amphiphiles. Since the fluorescence emissions from these amphiphiles are rather weak for observing the distribution of molecules at the surface, the cross-section images were taken in all cases. As are shown

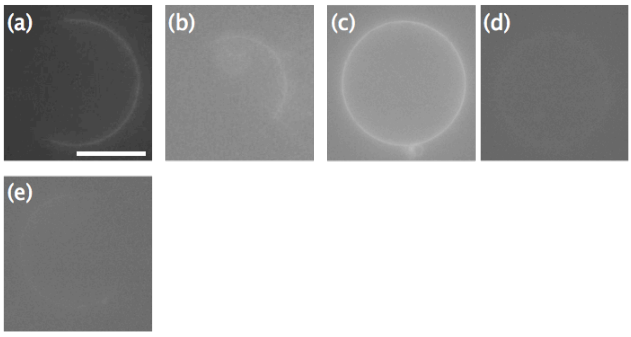

Figure 6. Fluorescence microscopic images of GUVs without fluorescent probes the presence of a) **1mer-bpy**, b) **1mer-2bpy**, c), d) **1mer-3bpy**, and e) **3mer-bpy**. DOPC/DPPC/Chol/multiblolck amphiphile = 40/40/20/10. λ_{ex} = 330-385 nm. Scale bar: 10 µm.

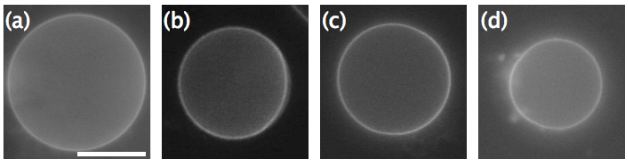

Figure 7. Fluorescence microscopic images of GUVs labelled by **BODIPY-Chol** in the presence of a) **1mer-bpy**, b) **1mer-2bpy**, c) **1mer-3bpy**, and d) **3mer-bpy**. DOPC/DPPC/Chol/multiblolck amphiphile = 40/40/20/10. λ_{ex} = 330-385 nm. Scale bar: 10 μm.

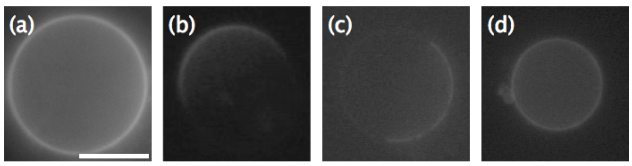

Figure 8. Fluorescence microscopic images of GUVs labelled by **BODIPY-Chol** in the presence of a) **1mer-bpy**, b) **1mer-2bpy**, c) **1mer-3bpy**, and d) **3mer-bpy**. DOPC/DPPC/Chol/multiblolck amphiphile = 40/40/20/10. λ_{ex} = 470-495 nm. Scale bar: 10 μm.

in Figure 6, GUVs containing **1mer-bpy, 1mer-2bpy**, **1mer-3bpy** and **3mer-bpy** could be clearly visualized under this condition, indicating that these amphiphiles are incorporated in the lipid bilayers. On the other hand, in the case of **1mer-4bpy**, no vesicle image was obtained under this condition, indicating that **1mer-4bpy** was not incorporated in the lipid bilayer with this composition. Importantly, in cases of **1mer-bpy, 1mer-2bpy**, and **3mer-bpy**, the cross-sectional images did not show a perfect circle, but arc-like architectures. In the case of **1mer-3bpy**, while a full circle image was observed for one of the vesicles, the other one shows very weak images. These result strongly suggest delocalization of these amphiphiles in Ld or Lo phases.

Fluorescence microscopic observation of DOPC/DPPC/cholesterol/multiblock-amphiphile GUVs in the presence of cholesterol labelled with BODIPY.

Then, we conducted the fluorescence microscopy of GUVs containing cholesterol labelled with boron-dipyrromethene (**BODPY-Chol**), which is known to delocalize in Lo phase consisting of DPPC and cholesterol. Upon excitation by UV lights (330-385 nm), the circle images of GUVs are found for all GUVs containing **1mer-bpy, 1mer-2bpy**, **1mer-3bpy** and **3mer-bpy** (Figure 7). Furthermore, when excitation was performed by visible lights (470-495 nm) corresponding to the excitation wavelengths of BODPY, GUVs containing **1mer-bpy** and **3mer-bpy** showed circle images, while those containing **1mer-2bpy** and **1mer-3bpy** showed arc-like architectures (Figure 8). UV lights excite both BODPY and multiblock amphiphiles, while the visible lights only excite BODPY and do not excite the multiblock amphiphiles. Thus, these results mean that **BODPY-Chol** is delocalized in both Lo and Ld phases in the case of

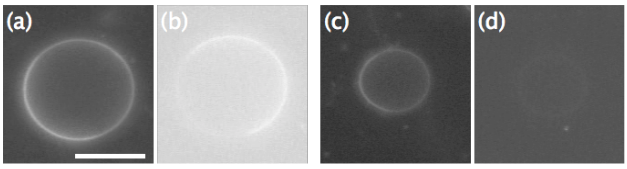

Figure 9. Fluorescence microscopic images of GUVs labelled by **NDB-DPPE** in the presence of a), b) **1mer-bpy** and c), d) **1mer-3bpy**. DOPC/DPPC/Chol/multiblolck amphiphile = 40/40/20/10. Excited by a), c) visible and b), d) UV (330-385 nm) lights, respectively. Scale bar: 10 μm.

GUVs containing **1mer-bpy** and **3mer-bpy**. Meanwhile, in cases of GUVs containing **1mer-2bpy** and **1mer-3bpy**, **BODPY-Chol** is considered to be localized in Lo phase, while **1mer-2bpy** and **1mer-3bpy** are considered to be localized in Ld phase.

Fluorescence microscopic observation of DOPC/DPPC/cholesterol/multiblock-amphiphile GUVs in the presence of DDPE labelled with NBD.

The above results clearly showed delocalization of **1mer-2bpy** and **1mer-3bpy** in Ld phase. However, it was still ambiguous whether **1mer-bpy** and **3mer-bpy** localize in Lo or Ld phase. Thus, we prepared GUVs containing dipalmitoylphosphatidylethanolamine labeled with 7-nitrobenz-2-oxa-1,3-diazol (**NBD-DPPE**), which is known to delocalize in Lo phase. NBD gives the emission upon excitation with visible lights, while excitation by UV lights hardly gives the emission. As a result, upon irradiation with visible lights, GUVs consisting of DOPC/DPPC/cholesterol/**1mer-bpy** (40/40/20/10) gave the circle images, where the intensity of the emissions is not homogeneous but segregated (Figure 9). This suggests that **NBD-DPPE** is delocalized in Lo phase. Upon excitation with UV lights, the opposite site of GUVs gave brighter images than those upon UV excitation. This means that **1mer-bpy** locates at the different phase from Lo phase, namely in Ld phase. In the case of **3mer-bpy,** probably due to the weak emission of **3mer-bpy**, such a clear contrast found in the case of **1mer-bpy** was not observed in the fluorescence images upon excitation with UV lights.

Confocal Fluorescence microscopic observation of DOPC/DPPC/cholesterol/multiblock-amphiphile GUVs in the

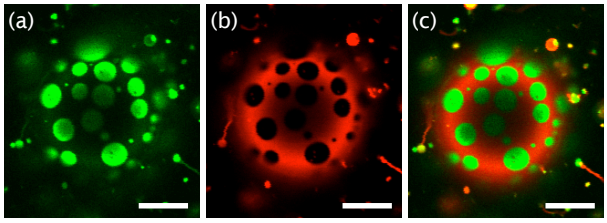

Figure 10. Confocal fluorescence microscopic images of GUVs labelled by **BODIPY-Chol** and **Rhodamin DHPE**. Observed by excitation of a) **BODIPY-Chol**, b) **Rhodamin DHPE**, and c) merged image of a) and b). DOPC/DPPC/Chol/multiblolck amphiphile = 40/40/20/10. Scale bar: 10 μm.

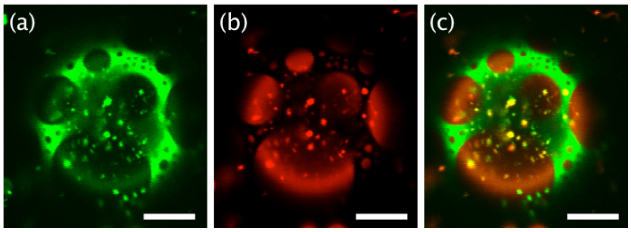

Figure 11. Confocal fluorescence microscopic images of GUVs consisting of DOPC/DPPC/Chol/**1mer-2bpy** = 40/40/20/10, observed by excitation of a) **BODIPY-Chol**, b) **Rhodamine-DHPE**, and c) merged image of a) and b). Scale bar: 10 μm.

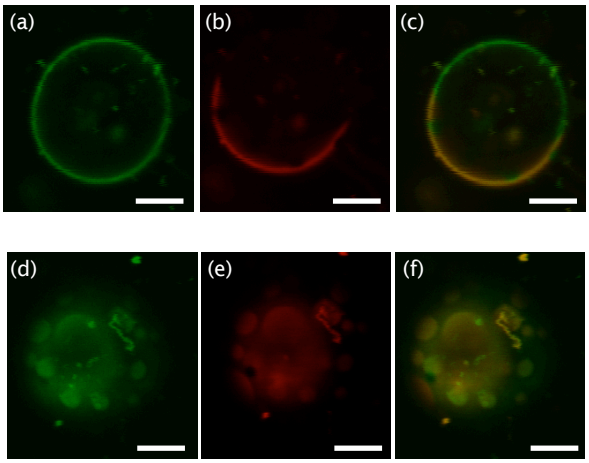

Figure 12. Confocal fluorescence microscopic images of GUVs consisting of DOPC/DPPC/Chol/**1mer-bpy** = 40/40/20/10, observed by excitation of a) d) **BODIPY-Chol**, b), e) **Rhodamin DHPE**, and c), f) merged image of a), c) and d), e). Scale bar: 10 μm.

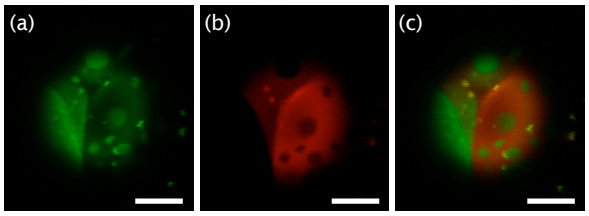

Figure 13. Confocal fluorescence microscopic images of GUVs consisting of DOPC/DPPC/Chol/**3mer-bpy** = 40/40/20/10, observed by excitation of a) **BODIPY-Chol**, b) **Rhodamin DHPE**, and c) merged image of a) and b). Scale bar: 10 μm.

presence of Rhodamine-DHPE and BODIPY-Chol.

Fluorescence microscopic observation of GUVs consisting of DOPC/DPPC/cholesterol/multiblock-amphiphile including **1mer-bpy** and **3mer-bpy** suggest delocalization of **BODPY-Chol** in both Lo and Ld phases. In order to confirm this effect, confocal fluorescence microscopic observation of GUVs was carried out for those including both **Rhodamine-DHPE** and **BODIPY-Chol**. Without multiblock amphiphiles, phase-separated GUVs are clearly observed by merging the images observed by excitation of rhodamine and BODPY moieties, respectively (Figure 10). Also in the case of GUV, including **1mer-2bpy**, similar images were obtained (Figure 11), indicating that **1mer-2bpy** does not influence on the phase-separation behaviour of DOPC/DPPC/cholesterol mixture. In contrast, in the case of GUVs containing **1mer** and **3mer**, excitation of **Rhodamine-DHPE** revealed the phase separated images (Figure 12). On the other hand, **BODIPY-Chol** showed distribution to whole GUVs, although some differences in the contrasts between two phases are observed (Figure 13). This is consistent with the observation in fluorescence microscopic images shown in Figure 7, indicating delocalization of **BODIPY-Chol** in both Lo and Ld phases.

Experimental

Materials.

DOPC, DPPC, BODIPY-Chol, and NBD-DPPE were purchased from Avanti Polar Lipids. Rhodamine-DHPE and was purchased from Molecular Probes. $CHCl_3$, CuI, glucose, methanol and tetrahydrofuran (THF) were purchased from Nacalai Tesque. $Pd(PPh_3)_4$ was purchased from Tokyo Chemical Industry. Dry triethylamine were purchased from Sigma-Aldrich. Deuterated solvents were purchased from Acros Organics. These commercial reagents were used without purification. Dry THF was purchased from Kanto Chemical and passed through sequential two drying columns on a Glass-Contour system just prior to use. Silica gel column chromatography was carried out with Chromatorex-NH-DM1020 silica (spherical, pH 9.5, particle size: 100 μm) purchased from Fuji Silysia Chemical. Deionized water (filtered through a 0.22 μm membrane filter, >18.2 MΩ cm) was purified in a Milli-Q system of Millipore Corp.

Instrumentation.

^{1}H nuclear magnetic resonance (NMR) spectra were recorded on a 400 MHz FT NMR Bruker BioSpin AVANCE III 400, where the chemical shifts were determined with respect to tetramethylsilane (TMS) or a residual non-deuterated solvent as an internal standard. High-resolution electrospray ionization (HR ESI) TOF MS spectra were recorded on a Bruker micrOTOF-Q II-S1 with MeOH as a solvent. Analytical thin layer chromatography (TLC) was performed on precoated, glass-backed silica gel (Merck 60 F254). Visualization of the developed chromatogram was performed by UV absorbance, Hanessian's stain or iodine. Fluorescent and phase contrast microscopy was performed with an Olympus IX-71 microscope, where a U-MWU2 mirror unit (excitation filter: 330–385 nm, emission filter: 420 nm, dichroic mirror: 400 nm) was used for fluorescence observation. On a slide glass, a coverslip was placed over the object through a 0.1-mm thick silicon-based spacer. UV-Vis absorption spectra were recorded on a JASCO V-530 UV-Vis spectrophotometer. Fluorescence spectra were recorded on a JASCO FP-6500 spectrophotometer.

Synthesis of 1mer-bpy, 1mer-2bpy, 1mer-3bpy, and 1mer-4bpy.

Synthesis of **1** and **2** were carried out following the procedures described in our previous paper.[14] To a degassed solution of **1**

(19.3 mg, 0.083 mmol) and **2** (106 mg, 0.185 mmol) in a mixture of dry THF (5.0 mL) and dry triethylamine (2.5 mL) were added Pd(PPh3)4 (24.1 mg, 0.020 mmol) and CuI (8.8 mg, 0.046 mmol) at 25 °C under Ar. After being stirred for 12 h at 25 °C, the resulting mixture was evaporated to dryness under reduced pressure. The residue was purified by silica gel chromatography (Chromatorex-NH-DM1020 silica) with a gradient from CH_2Cl_2 to CH_2Cl_2/MeOH (20/1) followed by size exclusion chromatography on a Japan Analytical Industry LC-9201 Recycling Preparative HPLC system with JAIGEL-1H and 2H columns with $CHCl_3$ as an eluent running at 3.5 mL min^{-1} to allow separation of **1mer-bpy** (57.6 mg, 0.051 mmol, 62% yield)**, 1mer-2bpy** (10.2 mg, 0.007 mmol, 9% yield), **1mer-3bpy** (6.6 mg, 0.004 mmol, 5% yield), and **1mer-4bpy** (0.6 mg, 0.3 μmol, 0.4% yield) as yellowish solids.

1mer-bpy: TLC (CH_2Cl_2/MeOH = 20/1) R_f = 0.60; ^{1}H NMR (400 MHz, $CDCl_3$ containing 0.03% TMS, 22 °C): δ = 8.65 (s, 2H), 7.75 (s, 2H), 7.49 (d, *J* = 8.8 Hz, 4H), 6.92 (d, *J* = 8.8 Hz, 4H), 4.17 (t, *J* = 4.8 Hz, 4H), 3.88 (t, *J* = 4.8 Hz, 4H), 3.75–3.59 (m, 56H), 3.05 (s, 2H), 2.20 (s, 6H) ppm; HR ESI-TOF MS (MeOH, positive mode): *m/z* = 1143.564 (calculated *m/z* on the basis of the monoisotropic mass of $C_{60}H_{84}N_2NaO_{18}$ $[M + Na]^+$ = 1143.562).

1mer-2bpy: TLC (CH_2Cl_2/MeOH = 20/1): R_f = 0.60; ^{1}H NMR (400 MHz, $CDCl_3$ containing 0.03% TMS, 22 °C): δ 8.69 (d, *J* = 1.6 Hz, 2H), 8.65 (d, *J* = 1.6 Hz, 2H), 7.79 (d, *J* = 2.0 Hz, 2H), 7.76 (d, *J* = 2.0 Hz, 2H), 7.50 (d, *J* = 8.4 Hz, 4H), 6.92 (d, *J* = 8.8 Hz, 4H), 4.17 (t, *J* = 4.8 Hz, 4H), 3.88 (t, *J* = 4.8 Hz, 4H), 3.75-3.60 (m, 56H), 2.92 (s, 2H), 2.21 (d, *J* = 2.8 Hz, 12H) ppm; HR ESI-TOF MS (MeOH, positive mode): *m/z* = 1373.635 (calculated *m/z* on the basis of the monoisotropic mass of $C_{76}H_{94}N_4O_{18}$: $[M + Na]^+$ 1373.646).

1mer-3bpy: TLC (CH_2Cl_2/MeOH = 20/1): R_f = 0.60; ^{1}H NMR (400 MHz, $CDCl_3$ containing 0.03% TMS, 22 °C): δ 8.69 (s, 4H), 8.65 (d, *J* = 1.6 Hz, 2H), 7.80 (t, *J* = 2.4 Hz, 4H), 7.77 (d, *J* = 1.6 Hz, 2H), 7.50 (d, *J* = 8.8 Hz, 4H), 6.92 (d, *J* = 9.2 Hz, 4H), 4.17 (t, *J* = 4.4 Hz, 4H), 3.88 (t, *J* = 4.8 Hz, 4H), 3.75-3.60 (m, 56H), 2.92 (s, 2H), 2.22 (d, *J* = 2.4 Hz, 12H), 2.21 (s, 6H) ppm; HR ESI-TOF MS (MeOH, positive mode): *m/z* = 1604.719 (calculated *m/z* on the basis of the monoisotropic mass of $C_{92}H_{104}N_6O_{18}$: $[M + Na]^+$ 1604.734).

1mer-4bpy: TLC (CH_2Cl_2/MeOH = 20/1): R_f = 0.60; ^{1}H NMR (400 MHz, $CDCl_3$ containing 0.03% TMS, 22 °C): *d* 8.71 (s, 6H), 8.67 (d, *J* = 1.6 Hz, 2H), 7.82 (d, *J* = 1.2 Hz, 6H), 7.78 (d, *J* = 1.6 Hz, 2H), 7.51 (d, *J* = 8.8 Hz, 4H), 6.94 (d, *J* = 8.8 Hz, 4H), 4.19 (t, *J* = 4.8 Hz, 4H), 3.90 (t, *J* = 4.8 Hz, 4H), 3.77-3.62 (m, 56H), 2.67 (s, 2H), 2.242 (s, 12H), 2.235 (s, 6H), 2.227 (s, 6H) ppm; HR ESI-TOF MS (MeOH, positive mode): *m/z* = 928.897 (calculated *m/z* on the basis of the monoisotropic mass of $C_{108}H_{114}N_8O_{18}$: $[M + 2Na]^{2+}$ 928.904).

Preparation of giant unilamellar vesicles.

A typical procedure is as follows. A $CHCl_3$/MeOH (2/1 v/v) solution of DOPC (2.0 mM, 18 μL) and a $CHCl_3$ solution of **1** or **2** (2.0 mM, 2.0 μL) were mixed in a glass test tube, and the resulting mixture was gently dried under Ar flow to produce thin lipid film. The film was subsequently dried under vacuum over 3 h and hydrated overnight with water (200 μL) at 37 °C. The final total lipids concentration was 0.20 mM.

Durham fermentation tube was treated with a mixture of chloroform and methanol (10 mL, 2:1) prior to use. Then to the tube was added a methanol solution of glucose (10 mM, 12 μL), chloroform solutions of DOPC (2 mM, 8 μL), DPPC (2 mM, 8 μL), cholesterol (2 mM, 4 μL), fluorescent probe (0.1 mM Rhodamine, 2μL or 0.1 mM BODIPY, 4 μL), multiblock amphiphile (0.2 mM, 20 μL). The resulting mixture was gently dried under Ar flow to produce thin lipid film. The film was subsequently dried under vacuum over 1.5 h and hydrated overnight with water (220 μL) at 37 °C.

Table 1 Distributions of multiblock amphiphiles and cholesterol in DOPC/DPPC/Chol/multiblock-amphiphile vesicles.

Compound	1mer-bpy	1mer-2bpy	1mer-3bpy	1mer-4bpy	3mer-bpy
Amphiphile	Ld	Ld	Ld	-	Ld
Cholesterol	Lo + Ld	Lo	Lo	-	Lo + Ld

Conclusions

Comparison of the spectroscopic properties of triblock amphiphiles **1mer-bpy, 1mer-2bpy**, **1mer-3bpy**, and **1mer-4bpy** suggest that the chromophores of these molecules, the diarylethyne and diarylbutadiyne units, could be separately excited to give emissions. This is likely reasonable considering the twisted geometry of these molecules at the bipyridine units, bearing methyl substituents at the *ortho* positions. Interestingly, upon increase in the polarity of the solvents, the longer molecule showed larger Stokes-shifts, i.e. up to 23 nm in the case of **1mer-4bpy**. Fluorescence microscopy displayed the distribution of these molecules in the phase-separated membranes with DOPC/DPPC/cholesterol. All the amphiphiles are found to be delocalized in Ld phase, except for **1mer-4bpy** which has apparently longer hydrophobic unit than the DOPC and DPPC (Table 1). Interestingly, **1mer-bpy** and **3mer-bpy**, having the shortest hydrophobic units, seemed to recruit cholesterol molecules into Ld phase. The length of the hydrophobic unit as well as its geometry may have some advantage on the interaction with cholesterol. Further study on this effect is in progress.

Conflicts of interest

There are no conflicts to declare.

Acknowledgements

This work was partially supported by Grant-in-Aid for Scientific Research B (16H04129 to KK), Yamada Science Foundation (KK), Grant-in-Aid for Scientific Research on Innovative Areas "π-

System Figuration (No.2601)" (26102001 to TM), JST PRESTO program "Molecular Technology and Creation of New Functions" (TM), and the Management Expenses Grants for National Universities Corporations from MEXT.

Notes and references

1 B. Alberts, A. Johnson, J. Lewis, D. Morgan, M. Raff, K. Roberts and P. Walter, in *Molecular Biology of the Cell*, 6th version, Garland Science, New York, 2014.
2 B. Hille, in *Ion Channels of Excitable Membranes*, 3rd Edn, Sinauer Associates, Sunderland, MA, 2001.
3 J. K. W. Chui, T. M. Fyles, *Chem. Soc. Rev.*, 2012, **41**, 148–175.
4 M. Barboiu and A. Gilles, *Acc. Chem. Res.*, 2013, **46**, 2814–2823.
5 G. W. Gokel and S. Negin, *Acc. Chem. Res.*, 2013, **46**, 2824–2833.
6 T. M. Fyles, *Acc. Chem. Res.*, 2013, **46**, 2847–2855.
7 J. Montenegro, M. Z. Ghadiri, and J. R. Granja, *Acc. Chem. Res.*, 2013, **46**, 2955–2965.
8 N. Sakai and S. Matile, *Langmuir*, 2013, **29**, 9031–9040.
9 A. V. Jentzsch and S. Matile, *Top. Curr. Chem.*, 2015, **358**, 205–239.
10 T. Muraoka, T. Shima, T. Hamada, M. Morita, M. Takagi andnd K. Kinbara, *Chem. Commun.*, 2011, **47**, 194–196.
11 T. Muraoka, T. Shima, T. Hamada, M. Morita, M. Takagi, K. V. Tabata, H. Noji and K. Kinbara, *J. Am. Chem. Soc.*, 2012, **134**, 19788–19794.
12 T. Muraoka, T. Endo, K. V. Tabata, H. Noji, S. Nagatoishi, K. Tsumoto, R. Li and K. Kinbara, *J. Am. Chem. Soc.*, 2014, **136**, 15584–15595.
13 T. Muraoka and K. Kinbara, *Chem. Commun.*, 2016, **52**, 2667.
14 T. Muraoka, K. Umetsu, K. V. Tabata, T. Hamada, H. Noji, T. Yamashita and K. Kinbara, *J. Am. Chem. Soc.*, 2017, **139**, 18016–18023.
15 S. L. Veatch, O. Soubias, S. L. Keller and K. Gawrisch, *Proc. Natl. Acad. Sci.*, 2007, **104**, 17650–17655.
16 J. Juhasz, F. J. Sharom and J. H. Davis, *Biochim. Biophys. Acta* 2009, **1788,** 2541–2552.
17 P. Uppamoochikkal, S. Tristram-Nagle and J. F. Nagle, *Langmuir*, 2010, **26**, 17363–17368.
18 J. Wolff, C. M. Marques and F. Thalmann, *Phys. Rev. Lett.*, 2011, **106**, 128104.
19 J. Joannis, P. S. Coppock, F. Yin, M. Mori, A. Zamorano and J. T. Kindt, *J. Am. Chem. Soc.*, 2011, **133**, 3625–3634.
20 K. Simons and E. Ikonen, *Nature*, 1997, **387**, 569–572.
21 E. London, *Curr. Opin. Struct. Biol.*, 2002, **12**, 480–486.
22 K. Simons and W. L C Vaz, *Annu. Rev. Biophys. Biomol. Struct.*, 2004, **33**, 269–95.
23 L. J. Pike, *J. Lipid Res.*, 2006, **47**, 1597–8.
24 D. Lingwood and K. Simons, *Science*, 2010, **327**, 46–50.
25 K. Sonogashira, Y. Tohda and N. Hagihara, *Tetrahedron lett.* **1975**, *50*, 4467–4470.

